Original Article

cyy-287, a novel pyrimidine-2,4-diamine derivative, inhibits tumor growth of EGFR-driven non-small cell lung cancer via the ERK pathway

Qianwen Zhang[1,†,*], Huijing Huang[2,†], Shuwen Zheng[1], Yelin Tang[2], Xiaodan Zhang[1], Qianqian Zhu[2], Zefeng Ni[2], Xiaohui Zheng[2], Kun Wang[2], Lehao Huang[2], Yunjie Zhao[2,*], Zhiguo Liu[2,*], and Jianchang Qian[1,*]

[1]Institute of Molecular Toxicology and Pharmacology, Wenzhou Medical University, Wenzhou 325035, China, and [2]Chemical Biology Research Center at School of Pharmaceutical Sciences, Wenzhou Medical University, Wenzhou 325035, China
[†]These authors contributed equally to this work.
*Correspondence address. Tel: +86-577-86689710; E-mail: zqwlovelove@126.com (Q.Z.) / Tel: +86-577-86689984; E-mail: aabye1100@aliyun.com (Y.Z.) / Tel: +86-577-86699892 (Z.L.); E-mail: lzgcnu@163.com (Z.L.) / Tel: +86-577-86699574 (J.Q.); E-mail: qianjc@wmu.edu.cn (J.Q.)

Abstract

In recent decades, EGFR-targeted tyrosine kinase inhibitors (TKIs) have been proven to be an effective therapy for EGFR-mutant non-small cell lung cancer (NSCLC). However, resistance to EGFR-TKIs limits their clinical application. In the present study, we investigate the antitumor effect and underlying mechanism of a novel pyrimidine-2,4-diamine derivative, cyy-287, in NSCLC. We find that cyy-287 has a high affinity for lung tissue and inhibits the proliferation of NSCLC cells. Interestingly, the significant suppression of migration and induction of apoptosis by cyy-287 are only observed in EGFR-driven but not in EGFR-wild-type (wt) cells. According to the RNA sequencing and KEGG enrichment analysis results, cyy-287 markedly inhibits the MAPK pathway in EGFR-driven PC9 cells, and western blot analysis results further indicate that cyy-287 selectively blocks the ERK pathway in EGFR-driven cells. Meanwhile, apoptosis induced by cyy-287 could be partially reversed by ERK pathway inhibition. Further experiment indicates that cyy-287 inhibits the EGFR pathway in both EGFR-driven and EGFR-overexpressing cells. Interestingly, it only induces apoptosis in EGFR-driven cells, not in EGFR-overexpressing cells. The growth of EGFR-driven cells is suppressed by cyy-287 *in vivo*, with fewer side effects. Our results suggest that cyy-287 may be a potential therapeutic drug with promising antitumor effects against NSCLC.

Key words   cyy-287, non-small cell lung cancer, EGFR, ERK

Introduction

Despite significant progress in diagnosis and clinical management, lung cancer remains the leading cause of cancer-related deaths worldwide, causing 1.79 million deaths in 2020 [1,2]. As one of the most common and invasive types of lung cancer, non-small cell lung cancer (NSCLC) accounts for 85% of all lung cancer cases [3]. More than 40% of newly diagnosed NSCLC cases will be in stage IV, and cytotoxic combination chemotherapy is recommended as the first-line therapy [4]. The generally used chemotherapy is a platinum-based combination of gemcitabine, taxane and vinca alkaloids, but the objective response rate is only 17%–32%, and the

median survival time is less than 1 year [5,6]. With the development of personalized therapy, targeted drugs have improved the survival of patients with NSCLC. Epidermal growth factor receptor (EGFR), one of the common receptor tyrosine kinases (RTKs), is a key cancer-causing driver mutation in NSCLC. Approximately 15% of the US, and 40% of Asian NSCLC cases harbor mutations in the EGFR kinase domain [7]. Although the majority of such patients initially benefited from treatment with the first-generation EGFR-targeted tyrosine kinase inhibitors (TKIs) gefitinib and erlotinib or the second-generation inhibitors afatinib and dacomitinib, there is still significant heterogeneity in the clinical course of patients with

EGFR-mutant lung cancers [8,9]. Their efficacy failed due to secondary mutation. Acquisition of EGFR-T790M is the most frequently identified resistance mechanism and is detected in tumor cells from more than 50% of patients after disease progression [10]. Unfortunately, despite the third-generation EGFR-TKIs, including osimertinib (AZD9291) and rociletinib (CO-1686), which have been approved to treat patients with EGFR-T790M, tolerance still occurs [11]. Moreover, some newly discovered cancer-related changes, such as abnormal expression of the transcription factors SOX2 and MYC, or HMGB1-mediated autophagy, present another challenge to current treatment strategies [12–14]. Therefore, it is imperative to find new therapeutic methods to target tumor cells and develop more effective drugs.

The mitogen-activated protein kinase (MAPK) family is a member of the serine/threonine protein kinase superfamily. To date, the known MAPKs mainly consist of p38 MAPK, extracellular signal-regulated kinase (ERK), and c-Jun NH2-terminal kinase (JNK). MAPKs play critical roles in regulating numerous cellular activities, including gene expression, cell growth, migration, differentiation, and apoptosis, which have made these proteins a priority for research related to many human diseases [15,16]. Among the numerous intracellular signaling pathways, the MAPK pathway is essential for the progression of tumorigenesis and development. As serine-threonine kinases, MAPKs can be activated by multiple cellular stressors and cytokines. The MAPK pathway is one of the key downstream pathways of RTKs and is usually abnormally activated in RTK-driven tumors. In NSCLC patients with EGFR mutations, the MAPK pathway is upregulated and plays an important role in cell survival [17]. Therefore, blocking MAPK may be a promising strategy for the treatment of EGFR-mutant NSCLC.

In the present study, we investigated the antitumor effect and mechanism of the newly synthesized compound cyy-287 in NSCLC. cyy-287 was found to inhibit the growth and proliferation of EGFR-driven NSCLC cells *in vitro* and *in vivo*. In addition, cyy-287 effectively suppressed migration and induced apoptosis via the ERK pathway in EGFR-driven cells. Our results suggest that cyy-287 has great potential as a new drug for the treatment of EGFR-mutant NSCLC.

Materials and Methods
Chemicals and antibodies
cyy-287 was synthesized as described in Supplementary Figure S1 by our laboratory, and the purity was ≥ 98%. For the characterization of compounds, ^{1}H NMR, ^{13}C NMR, electrospray ionization-mass spectrometry (ESI-MS), and high-resolution mass spectrometry (HRMS) techniques were applied. The MEK inhibitor UO126 (A1337), JNK inhibitor SP600125 (A4604), and p38 inhibitor SB203580 (A8254) were purchased from APExBIO (Houston, USA). Inhibitors were dissolved in DMSO as a 20 mM stock solution and were diluted before assays. MTS reagent was from Promega (Madison, USA), propidium iodide dye was from Sigma (St Louis, USA), Annexin V-FITC Apoptosis Detection Kit was from BD (Franklin Lakes, USA), Transwell was from Costar (New York, USA) and recombinant human EGF was from Peprotech (London, UK). Antibodies against cyclin A2, cyclin B1, cyclin D1, c-Myc, GAPDH, vimentin, E-cadherin, Slug, CL-PARP, p-ERK (Thr202/Tyr204), ERK1/2, p-p38 (Thr180/Tyr182), p38, p-JNK1/2 (Thr183/Tyr185), JNK1/2, p-EGFR (Tyr1068) and EGFR were purchased

from Cell Signaling Technology (Boston, USA).

Cell culture
H1975 cell line was obtained from American Type Culture Collection (ATCC, Manassas, USA). H1299, H292 and H441 cell lines were obtained from the Cell Bank of Chinese Academy of Sciences (Shanghai, China). PC9 cell line was obtained from European Collection of Cell Cultures (ECACC, Salisbury, UK). Cells were cultured in RPMI 1640 medium (Gibco, Carlsbad, USA) containing 10% FBS (Sigma) in a 37°C incubator with 5% CO_2.

Cell viability assay and drug combination index (CI)
Cells were seeded in 96-well plates (5%–10% confluence) and incubated for 48 or 72 h with different concentrations of cyy-287 before measurement using MTS reagent (Promega) according to the manufacturer's instructions. To obtain the CI, cells were seeded in 96-well plates (5%–10% confluence) and then incubated for 72 h with different concentrations of cyy-287, UO126 or cyy-287 combined with UO126 (the ratio is 1:1) before MTS assay. The CI was calculated using CompuSyn software (www.combosyn.com). Synergism is described when the scale of CI is 0–1, while antagonism is determined when CI is more than 1.

Colony formation assay
Cells were seeded in 12-well plates at 800 cells/well and then exposed to different concentrations of cyy-287 or gefitinib for 24 h. Then, the drugs were removed, and the cells were cultured with fresh media for another 8 days. The cell colonies were fixed with 4% paraformaldehyde for 20 min, stained with 0.5% crystal violet solution (Sigma) for 30 min, and counted.

Cell cycle and apoptosis detection by flow cytometry
Cells were seeded in 6-well plates (20%–25% confluence) and exposed to different concentrations of cyy-287 or gefitinib for 24 h. Apoptosis was assessed using the Annexin V-FITC Apoptosis Detection Kit (BD, Franklin Lakes, USA) according to the manufacturer's instructions. For the cell cycle, the cells were harvested and fixed with 70% ethanol for 24 h at 4°C. After two times wash with phosphate-buffered solution (PBS) and incubation with RNase A in a water bath at 37°C for 30 min, the cells were stained with propidium iodide (50 μg/mL; Sigma) for 10 min. Both cell cycle distribution and apoptosis were analyzed by flow cytometry on a BD FACSCalibur flow cytometer.

Western blot analysis
For the standard assay of inhibitory effects, cells plated at predetermined density in 12-well culture plates were treated with cyy-287 or gefitinib at indicated doses for indicate time, lysed in NuPAGE-LDS lysis buffer (Invitrogen, Carlsbad, USA). The protein samples were then subject to 10% SDS-PAGE and then transferred to a 0.45 μM nitrocellulose filter membranes (PALL, New York, USA). Membranes were blocked at room temperature with freshly prepared 5% skim milk powder for 2.5 h, followed by incubation with various antibodies (1:1000) as indicated overnight at 4°C. Then membranes were incubated with the corresponding HRP-conjugated secondary antibody (1:10,000; Jackson, West Grove, USA) for 2 h. After washing by TBST for three times, protein bands on membranes were detected using an enhanced chemiluminescence detection kit (Millipore, Billerica, USA) and the protein gray

value was quantified by ImageJ software (https://imagej.nih.gov/ij/). GAPDH was used as the loading control.

Sequencing transcriptomics

Cells were harvested after treatment with cyy-287 (3 μM) for 24 h, and total RNA was extracted for RNA sequencing. Illumina sequencing was performed by Metware Biotech (Wuhan, China) using the Illumina Nova-seq 6000 (Illumina, San Diego, USA). DESeq2 was applied for differential gene expression analysis. Feature counts were used to count the read numbers. The resulting P values were adjusted by the Benjamini-Hochberg approach to control for a false discovery rate (FDR). Genes with |log2(fold change)| ≥ 1 and FDR < 0.05 were considered to be differentially expressed. The differentially expressed genes were further analyzed with KEGG (http://www.genome.jp/kegg/).

Wound healing and Transwell migration assay

After the cells were grown to 100% confluence, mechanical injury was created using a sterile 200-μL pipette tip, and the debris was washed away with PBS. Cells were incubated in RPMI 1640 medium (Gibco) containing 0.5% FBS (Sigma) with different concentrations of cyy-287 for 16 h. Images were captured under a NIB610 microscope (Nexcope, Guangzhou, China) at 0 and 16 h after scratching at 100 × magnification.

For Transwell migration assay, PC9 ($8 × 10^4$), H1975 ($10 × 10^4$), and H1299 ($20 × 10^4$) cells suspended in 200 μL serum-free medium were added to the upper chamber of a Transwell system (Corning, NY, USA) with different concentrations of cyy-287 or gefitinib. Then, the cells were allowed to migrate for 20 h toward 10% serum medium in the lower chamber. The migrated cells were stained with crystal violet and counted under the NIB610 microscope in six representative viewing fields at 400 × magnification.

In vivo tumor growth inhibition, evaluation of serum levels of ALT, AST and creatinine and Ki-67 staining

Animal studies were approved by the Institutional Animal Care and Use Committee (IACUC) of Wenzhou Medical University. BALB/c nude mice (4-6 weeks old) were purchased from Beijing Vital River Laboratory Animal Technology Co., Ltd (Beijing, China). Mice were bred in the animal center at 20–22 °C and 50%–60% humidity with standard 12 h light/dark cycles. PC9 cells ($6 × 10^7$ cells/mL) were injected subcutaneously into the right flanks of the mice. The tumors were staged at an initial tumor volume of 80 to 100 mm³ and randomized into treatment groups ($n = 6$). cyy-287 (salt form) and gefitinib were formulated in saline or ethanol-Tween-80-saline (1:1:6), respectively. Mice were dosed intraperitoneally once a day. Tumor growth was monitored and tumor volume was calculated using the formula: $V = L × W^2/2$, where V is volume, L is length, and W is width of the tumor. Blood was collected after the mice were sacrificed. After centrifugation, the supernatant was used to test the concentration of ALT, AST or creatinine with ALT/GPT, AST/GOT, or creatinine assay kits (Jiancheng Bioengineering Institute, Nanjing, China), respectively. For Ki-67 staining, tumor slides were deparaffinized, rehydrated, and permeabilized with 1% Triton X-100. Antigens were retrieved with 1 mM Tris/EDTA (pH 9.0) under microwave heating for 20 min and then blocked with 5% BSA in TBS and 0.3 M glycine, and then probed using anti-Ki-67 antibody. Images were acquired and analyzed by using a Pannoramic 250 FLASH scanner (3D HISTECH, Budapest, Hungary).

Sample preparation and tissue distribution of cyy-287

Kunming (KM) mice were purchased from Beijing Vital River Laboratory Animal Technology Co., Ltd (Beijing, China). The mice were sacrificed by cervical dislocation after cyy-287 (15 mg/kg) administration by intraperitoneal (i.p.) route for approximately 4 h (peak time), organs (heart, liver, spleen, lung, kidney) were surgically removed within 20 min. Then, the organs were homogenized in physiological saline (1:4 w/v). After centrifugation at 16,200 g for 10 min, 100 μL supernatant was collected and mixed with 200 μL acetonitrile and 20 μL diazepam (100 ng/mL). Then, the mixture was vortexed for 2 minutes and centrifuged at 16,200 g for 10 minutes, and 6 μL of the supernatant was injected into the ultra-performance liquid chromatography-tandem mass spectrometry (UPLC-MS/MS) (XEVO TQD; Waters, Millipore, Bedford, USA) system for the analysis of cyy-287.

Statistical analysis

Data processing and statistical analysis were performed with Microsoft Excel and GraphPad Prism 8 (GraphPad Software, La Jolla, USA). Data are expressed as the mean ± SD (standard deviation of triplicate determinations). Student's *t*-test or one-way analysis of variance was used to compare the different groups. $P < 0.05$ was considered statistically significant.

Results

cyy-287 has high affinity for lung tissue and inhibits cell growth in NSCLC

The selective distribution of an antitumor compound in the target organ determined its therapeutic effect and cell toxicity, so we first measured the distribution of cyy-287 (Figure 1A) *in vivo*. The results showed that cyy-287 was distributed mainly in the lung, kidney and blood after intraperitoneal injection (Figure 1B), which indicated that cyy-287 had high affinity for the lung tissue. To investigate the antiproliferative activity of cyy-287 in human NSCLC cell lines, a panel of five NSCLC cell lines was treated with different concentrations of cyy-287 for 48 h. The MTS assay results showed that cyy-287 inhibited the proliferation of all five NSCLC cell lines (Figure 2A). Interestingly, cyy-287 had better antiproliferative activity in EGFR-driven PC9 and H1975 cells, with IC$_{50}$ values of 1.11 ± 0.01 and 1.66 ± 0.05 μM, respectively (Table 1). Consistently, cyy-287 had superior colony formation inhibition in PC9 and H1975 cells than in EGFR-wild-type (wt) H1299 cells (Figure 2B). Then, we assessed the effects of cyy-287 on the cell cycle in these three NSCLC
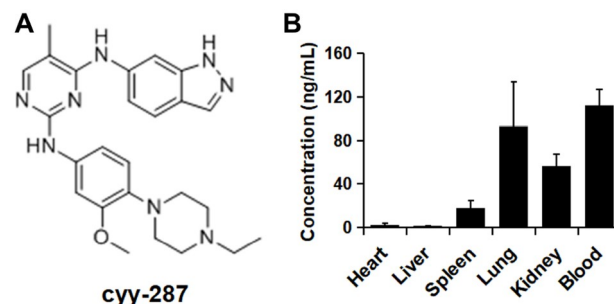
Figure 1. The structure and tissue distribution of cyy-287 (A) The chemical structure of cyy-287. (B) Mean concentration of cyy-287 in various tissues (heart, liver, spleen, lung, kidney) and blood at 4 h after i.p. administration of 15 mg/kg cyy-287 in mice. Data are shown as the mean ± SD ($n = 4$).

Table 1. IC$_{50}$ values of cyy-287 against various human NSCLC cell lines

Cell lines	IC$_{50}$ (µM)*
PC9 (EGFR L858R +)	1.11 ± 0.01
H1975 (EGFR T790M +)	1.66 ± 0.05
H1299 (EGFR-wt)	4.61 ± 0.50
H292 (EGFR-wt)	4.85 ± 0.32
H441 (EGFR-wt)	4.55 ± 0.42

*Data are presented as the mean ± standard deviation.

cell lines. As expected, cyy-287 induced G2/M arrest in a dose-dependent manner in PC9, H1975 and H1299 cells (Figure 2C). Similarly, cyy-287 had better G2/M arrest induction in PC9 and H1975 cells than in H1299 cells, whereas the first-generation EGFR inhibitor gefitinib arrested only PC9 (EGFR L858R +) cells at G0/G1 phase, correlating with a dose-dependent suppression of cell cycle-related or cell proliferation-related cyclin B1, cyclin D1 and c-Myc levels in three NSCLC cell lines (Figure 2D). Collectively, these results demonstrated that cyy-287 could inhibit the growth of NSCLC cells but had better growth suppression in EGFR-driven cells.
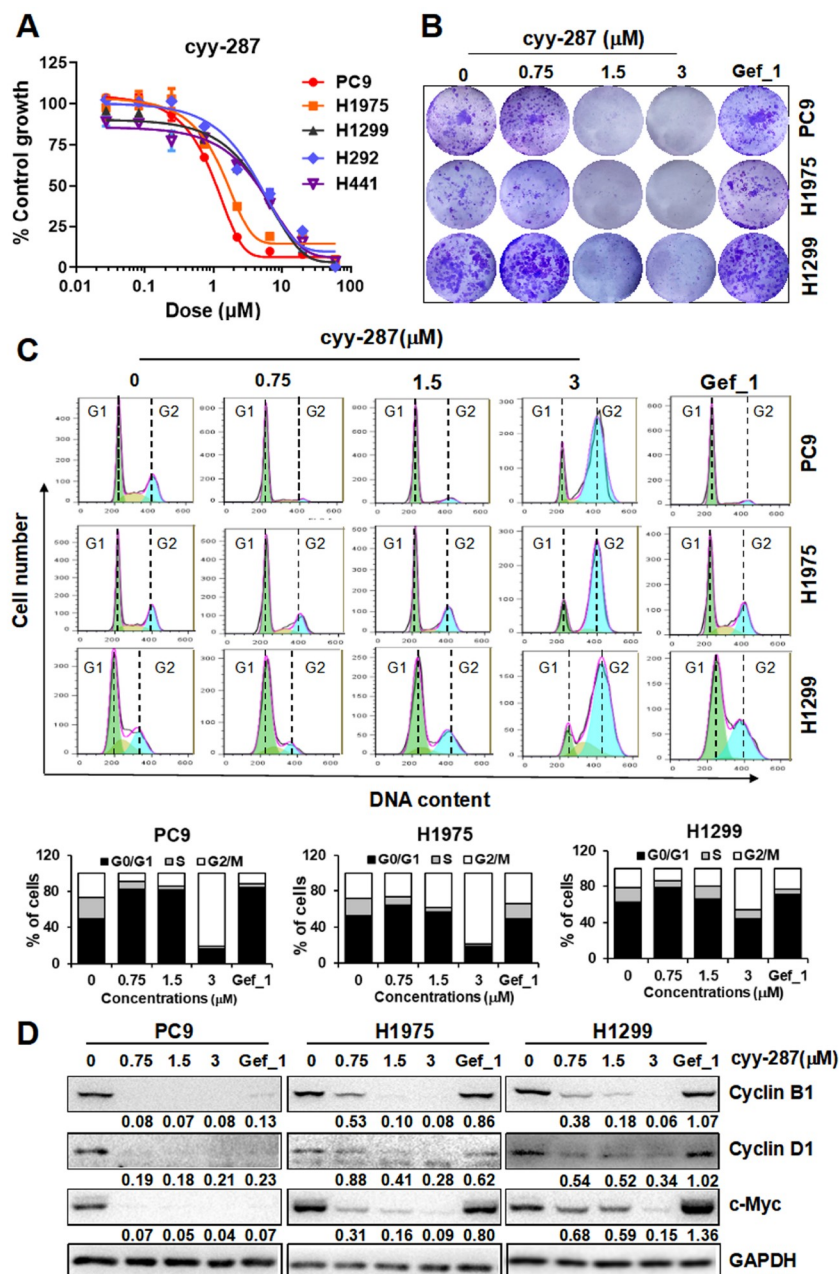
Figure 2. cyy-287 inhibits cell proliferation and induces cell cycle arrest in NSCLC cells (A) The indicated cell lines were treated with various doses of cyy-287 for 48 h, and the curves were plotted. (B) Colony formation assay in lung cancer cells treated as indicated. (C) Cells were treated as indicated for 24 h, and then PI staining analysis was conducted to analyze the cell cycle distribution by flow cytometry. (D) Quantified data of (C). (E) Cells were treated as indicated for 24 h and then subject to western blot analysis, and the grayscale value of each blot was quantified.

cyy-287 suppresses cell metastasis via EMT inhibition in EGFR-driven NSCLC cells

Lung adenocarcinoma is well known for its high incidence of metastasis and death. We then examined the effect of cyy-287 on tumor cell migration and metastasis. The wound healing assay revealed that cyy-287 resulted in a dose-dependent inhibition of cell migration in EGFR-driven PC9 cells but not in EGFR-wt H1299 cells (Figure 3A,B). Consistently, cyy-287 inhibited cell metastasis in a dose-dependent manner in PC9 and H1975 cells but not in H1299 cells as measured by Transwell invasion assay, and cyy-287 resulted in better inhibition of cell metastasis than gefitinib (Figure 3C,D). Increasing evidence indicates that aberrant activation of the embryonic programmed 'epithelial–mesenchymal transition' (EMT) promotes tumor cell invasion and metastasis [18]. Thus,

we performed western blot analysis to detect EMT-related protein level changes after cyy-287 treatment. The results showed that cyy-287 resulted in profound inhibition of Vimentin (mesenchymal marker) and Slug (transcription factor during EMT) in PC9 and H1975 cells but had little effect on H1299 cells; however, cyy-287 did not upregulate E-cadherin (epithelial marker) protein level in H1975 cells (Figure 3E). These results collectively suggested that cyy-287 selectively suppressed the aggressiveness of EGFR-driven NSCLC cells.

cyy-287 induces apoptosis in EGFR-driven NSCLC cells

To further investigate the effect of cyy-287 on the physiological functions of NSCLC cells, we assessed the effects of cyy-287 on cell death. cyy-287 treatment (0.75, 1.5 or 3 μM) resulted in apoptotic
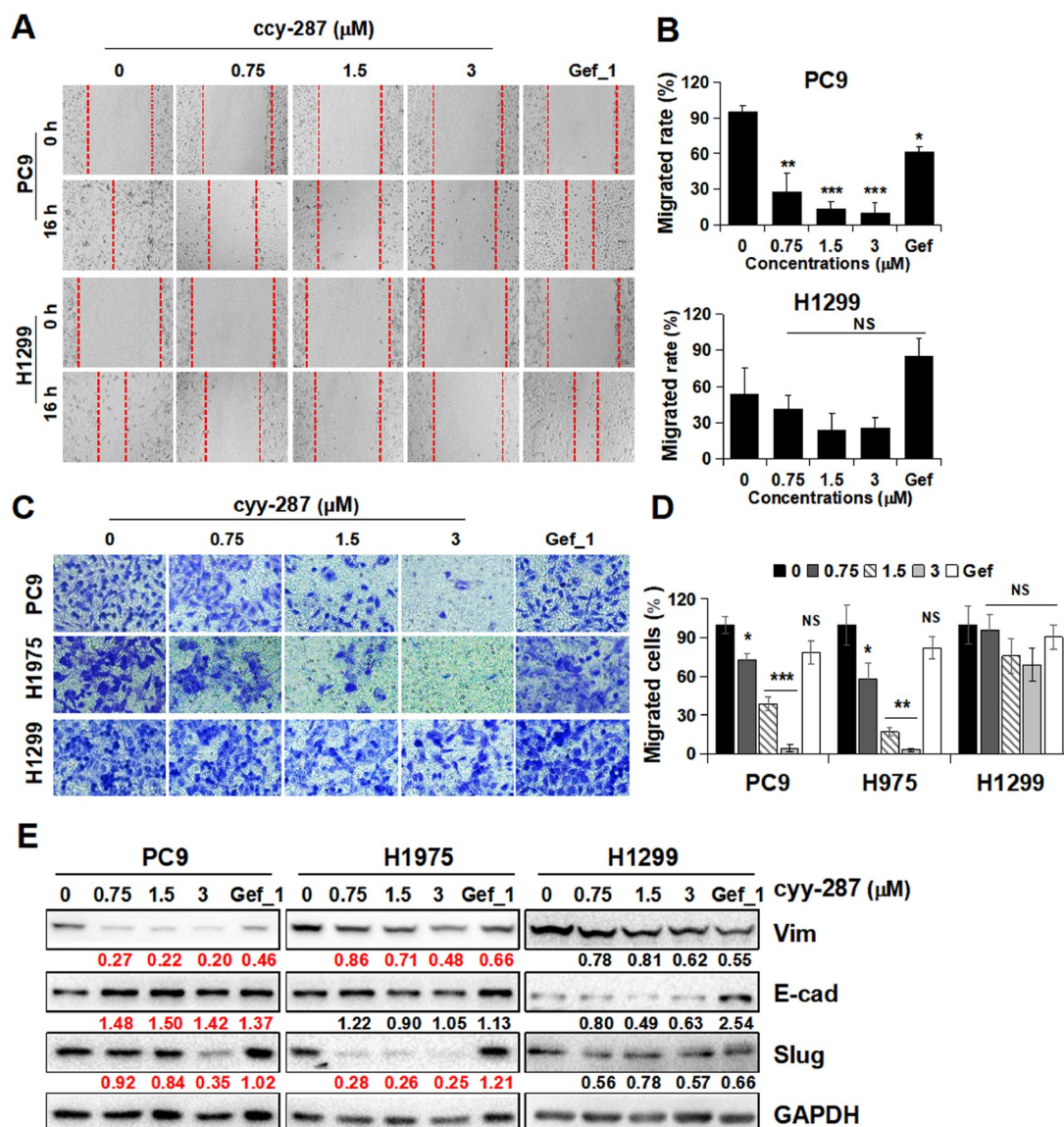
Figure 3. cyy-287 inhibits cell migration and EMT of EGFR-driven cells (A) Wound healing assay was used to determine the effect of cyy-287 on the migration of PC9 and H1299 cells, and the percentage of migrated cells is displayed (B). (C) Transwell assays were used to measure the effect of cyy-287 on the migration of lung cancer cells, and the percentage of migrated cells is displayed in (D). (E) Cells were treated as indicated for 24 h and then subject to western blot analysis and the grayscale value of each blot was quantified. Data are expressed as the mean ± SD. *$P < 0.05$, **$P < 0.01$, ***$P < 0.001$ compared with the control group. NS, no significance.

morphological changes, such as shrinkage, rounding and cytoplasmic budding, in PC9 and H1975 cells in a dose-dependent manner, but gefitinib did not. Interestingly, H1299 cells did not have any morphological changes and showed only a slight reduction in cell number (Figure 4A). Meanwhile, cyy-287 induced apoptosis in a dose-dependent manner, with apoptosis rates up to 59.9% (PC9) and 46.9% (H1975). However, almost no apoptotic cells were detected in H1299 cells, which was in accordance with the results of the morphological changes above (Figure 4B,C). Similarly, western blot analysis results demonstrated that cyy-287 induced apparent accumulation of PARP cleavage in PC9 and H1975 cells but not in

H1299 cells (Figure 4D). Taken together, these results suggested that cyy-287 selectively triggered apoptosis in EGFR-driven NSCLC cells in a dose-dependent manner.

cyy-287 induces apoptosis by blocking the ERK pathway in EGFR-driven NSCLC cells

To determine which pathway mainly contributes to the apoptosis induced by cyy-287 in EGFR-driven cells, we performed RNA-seq analysis of total RNA extracted from PC9 cells treated with or without cyy-287. The results showed that cyy-287 treatment significantly triggered differential gene expression (Figure 5A),
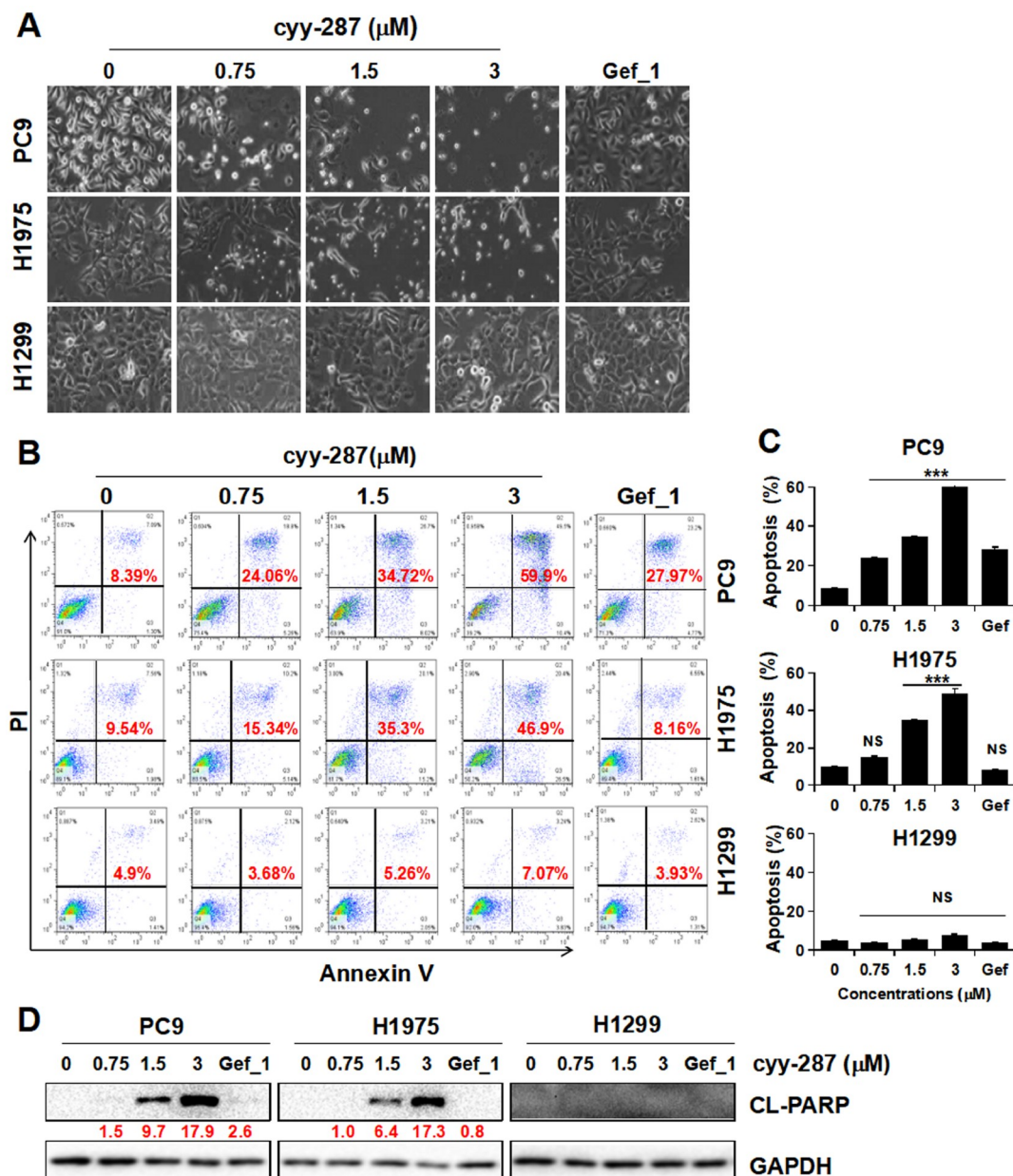
Figure 4. cyy-287 induces apoptosis in EGFR-driven cells (A) Cells were treated as indicated for 24 h, and morphological changes in apoptotic cells were observed (×100 magnification). (B) Cells were exposed to cyy-287 or gefitinib as indicated for 24 h, and Annexin V-FITC/PI staining analysis was conducted to evaluate the percentage of apoptotic cells by flow cytometry. (C) Quantitative data of (B). (D) Cells were treated as indicated for 24 h and then subject to western blot analysis, and the grayscale value of each blot was quantified. Data are expressed as the mean ± SD. ***$P < 0.001$, ****$P < 0.0001$ compared with the control group. NS, no significance.

with 1816 upregulated genes and 1782 downregulated genes (Figure 5B). In addition, we found that cyy-287 blocked the MAPK signaling pathway via KEGG pathway enrichment analysis (Figure 5C). To

further confirm the role of the MAPK signaling pathway in the three cell lines, we performed a western blot analysis. The results showed that cyy-287 treatment decreased the expression levels of p-JNK and
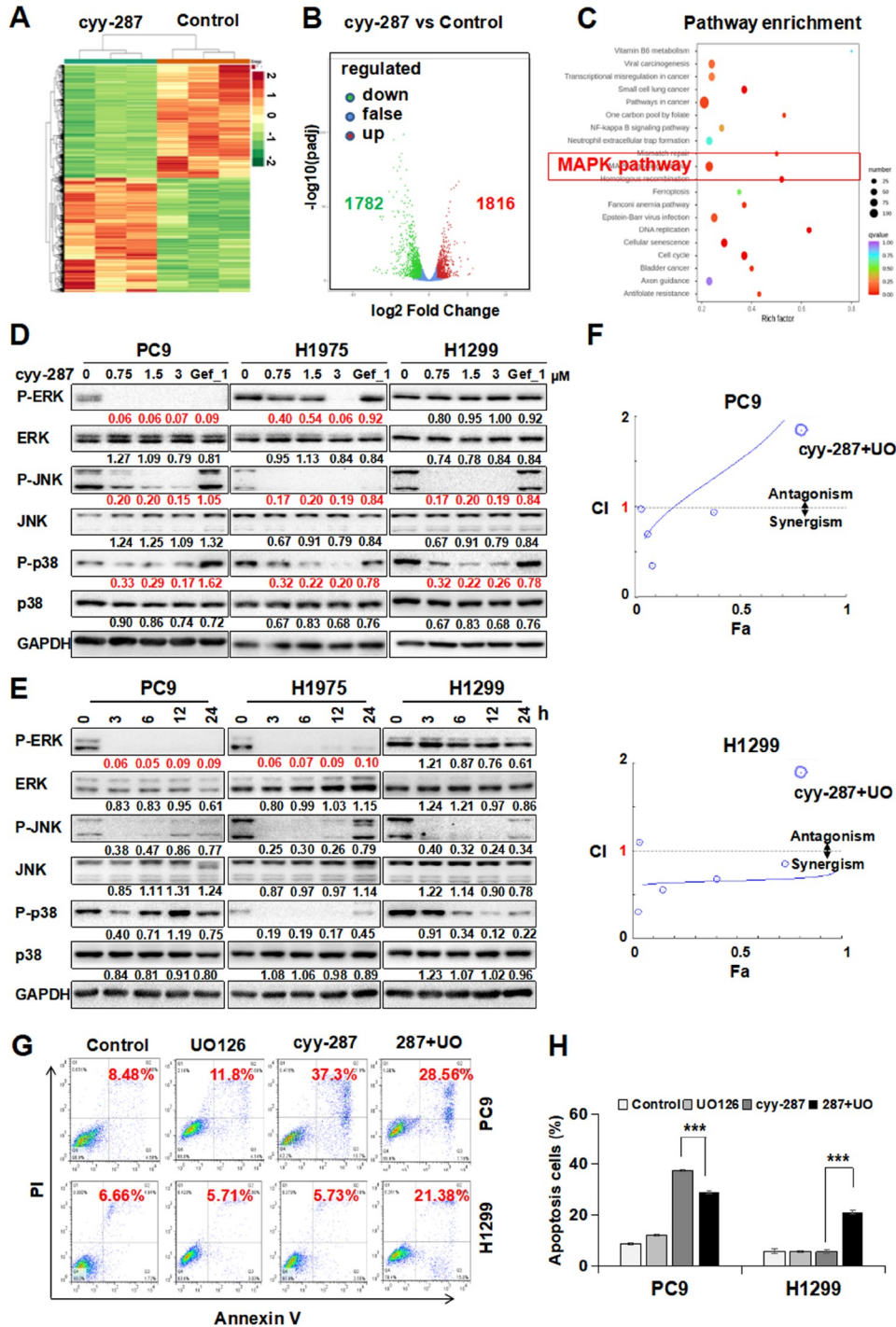
Figure 5. cyy-287 induces apoptosis in PC9 cells by ERK inhibition (A) Heatmap of significantly altered transcripts in PC9 cells treated with cyy-287 (3 μM) for 24 h. (B) Volcano plot showing differential gene expression of cyy-287-treated (3 μM) PC9 cells versus control cells (log2-transformed). (C) KEGG pathway enrichment analysis was performed in PC9 cells treated with cyy-287 (3 μM). (D) Cells were treated as indicated for 24 h and then subject to western blot analysis. (E) Cells were exposed to cyy-287 (3 μM) for various times as indicated and then subject to western blot analysis, and the grayscale value of each blot was quantified. (F) Combination index (CI) plot. (G) Apoptosis levels were analysed by the Annexin V-FITC/PI staining assay with or without UO126 (10 μM) pretreatment prior to cyy-287 (3 μM) exposure for 24 h. (H) Quantitative data of (G). Data are expressed as the mean ± SD. ***$P < 0.001$ compared with the control group.

p-p38 in all three cell lines in a dose-dependent manner, with no alteration of total JNK, p38 or ERK. However, cyy-287 did not alter p-ERK expression in H1299 cells (Figure 5D), implying a more prominent involvement for p-ERK in cyy-287-mediated differential cell apoptosis between EGFR-driven and EGFR-wt cells. Consistent with this, cyy-287 blocked p-ERK expression in a time-dependent manner in PC9 and H1975 cells but not in H1299 cells (Figure 5E). Then, we further examined apoptosis induced by cyy-287 in the presence of the MEK inhibitor UO126 and/or the p38 inhibitor SB203580 and/or the JNK inhibitor SP600125. We found that the combination index (CI) of cyy-287 combined with UO126 was more than 1 in most cases in PC9 cells, while the CI was less than 1 all the time in H1299 cells, which means that cyy-287 has antagonistic effects with UO126 on PC9 cells but synergistic effects on H1299 cells (Figure 5F). Meanwhile, the flow cytometry results showed that PC9 cell apoptosis level was decreased in the cyy-287 + UO group compared with that in the cyy-287 + group, but H1299 cell apoptosis level was increased in the (cyy-287 + UO) group, which indicated that cyy-287-induced cell apoptosis was mainly by ERK pathway inhibition in PC9 cells, yet the ERK pathway was incapable of triggering cell apoptosis in H1299 cells treated with cyy-287 (Figure 5G,H). Additionally, PC9 cell apoptosis level was increased in the cyy-287 + SB group and decreased in the cyy-287 + SP group compared with that in the cyy-287 + group, but H1299 cell apoptosis levels showed no significant changes in the cyy-287 + SB and cyy-287 + SP groups (Supplementary Figure S2). These results collectively suggested that the ERK pathway played an important role in cyy-287-mediated differential cell apoptosis between EGFR-driven and EGFR-wt NSCLC cells.

cyy-287 blocks EGFR expression in EGFR-driven NSCLC cells

To determine whether EGFR is involved in the apoptosis induced by cyy-287 in EGFR-driven cells, we assessed the effects of cyy-287 on EGFR expression in these three cell lines. Western blot analysis results demonstrated that cyy-287 blocked not only phosphorylated EGFR expression but also total EGFR expression in a dose-dependent manner in PC9 and H1975 cells but not in H1299 cells (Figure 6A). Additionally, although cyy-287 could block EGF-induced p-EGFR and p-ERK expression in a dose-dependent manner in H1299 cells, it had a stronger p-EGFR and p-ERK expression inhibition, including EGF-induced and basic protein expression in PC9 cells, which was in accordance with our results above (Figure 6B). Interestingly, we found that cyy-287 significantly blocked p-EGFR and p-ERK protein expression in H292 cells (Figure 6C), which had relatively higher p-EGFR expression level than H1299 cells but not EGFR-driven cells. However, cyy-287 only decreased c-Myc protein expression without inducing PARP cleavage in H292 cells (Figure 6D). The above results indicated that cyy-287 only induced cell death in EGFR-driven cells, not in EGFR-overexpressing cells, by inhibiting the EGFR pathway.

cyy-287 inhibits *in vivo* tumor growth of EGFR-driven cells

To evaluate the therapeutic effect of cyy-287 *in vivo*, we conducted an efficacy study of cyy-287 in EGFR-driven lung cancer models. Daily treatment with 15 and 5 mg/kg cyy-287 by i.p. injection produced a dose-dependent tumor inhibition in PC9 *in vivo* models, but not with comparable efficacy by 15 mg/kg gefitinib (Figure 7A).

cyy-287 produced a more profound tumor inhibition in H1975 *in vivo* models than gefitinib (Supplementary Figure S3). In addition, HE staining and Ki-67 staining results showed that the 15 mg/kg cyy-287 treatment group had more prominent apoptosis and necrosis and fewer Ki-67-positive tumour cells than the vehicle group (Figure 7B,C). Similarly, western blot analysis results demonstrated that cyy-287 blocked p-EGFR, p-ERK and cyclin D1 expressions in the tumours (Figure 7D). Finally, we evaluated the toxic effects of cyy-287 *in vivo*. The results showed that cyy-287 did not significantly reduce the body weight of mice or increase the concentration of ALT, AST and creatine in the blood (Figure 7E–H). These results collectively demonstrated that cyy-287 could inhibit tumour growth in EGFR-driven tumour models *in vivo* with minimal toxic effects.

Discussion

As one of the most common and invasive types of lung cancer, nearly two-thirds of NSCLC patients have local or distant metastasis at diagnosis with a poor prognosis, and the global 5-year survival rate is approximately 5% [19]. In the past few decades, it has been determined that the activation of EGFR is closely related to the genesis and progression of NSCLC [8,9]. Treatment with EGFR-TKIs has been the first-line treatment for NSCLC patients harboring activating EGFR mutations [20–22]. Studies have shown that the approval of targeted therapy, especially the clinical application of EGFR-TKIs, significantly reduces the incidence-based mortality of NSCLC [1]. Although the benefits of EGFR-TKIs are substantial, cancer will relapse within 1-2 years due to acquired resistance, mainly caused by a gatekeeper mutation, such as T790M [10]. To resolve this problem, covalently binding third-generation EGFR-TKIs selectively targeting T790M have been evaluated for the treatment of patients with advanced EGFR-mutated NSCLC [23]. However, resistance to osimertinib has again become a major obstacle [11]. Thus, acquired resistance to EGFR-TKIs has always been an impending problem for the clinical treatment of lung cancer.

Here, we first demonstrated that cyy-287, a novel pyrimidine-2,4-diamine derivative, had a strong inhibitory effect on the proliferation of human NSCLC cells in a dose-dependent manner *in vitro* (Figure 2A,B). The IC_{50} values of cyy-287 in EGFR-driven cell lines (< 2 μM) were less than half of those in EGFR-wt cell lines (> 4 μM) (Table 1), which suggested that cyy-287 is more effective in EGFR L858R + and EGFR T790M NSCLC cells. Cell cycle analysis revealed that cyy-287 induced G2/M arrest in a dose-dependent manner in NSCLC cells (Figure 2C). Meanwhile, the subsequent experiments in the xenograft tumor model showed consistent results: a significant reduction in tumor volumes and Ki-67-positive cells in the cyy-287 (15 mg/kg) group (Figure 7A–C). We did not observe any obvious signs of toxic side effects or changes in body weight in the cyy-287-treated groups (Figure 7E–H). Although the efficacy of cyy-287 in the PC9 *in vivo* model was not as good as that of gefitinib (Figure 7A), the anti-tumor effect of cyy-287 in the H1975 *in vivo* model was better than that of gefitinib (Supplementary Figure S3A). All these data indicate that cyy-287 has a good antitumor effect in EGFR-driven NSCLC cells.

Most patients with advanced lung cancer die of tumor metastasis. EMT is a critical factor influencing tumor metastasis. EMT is a complex multistep event characterized by the downregulation of the epithelial marker cytokeratin and the acquisition of fibroblast-like
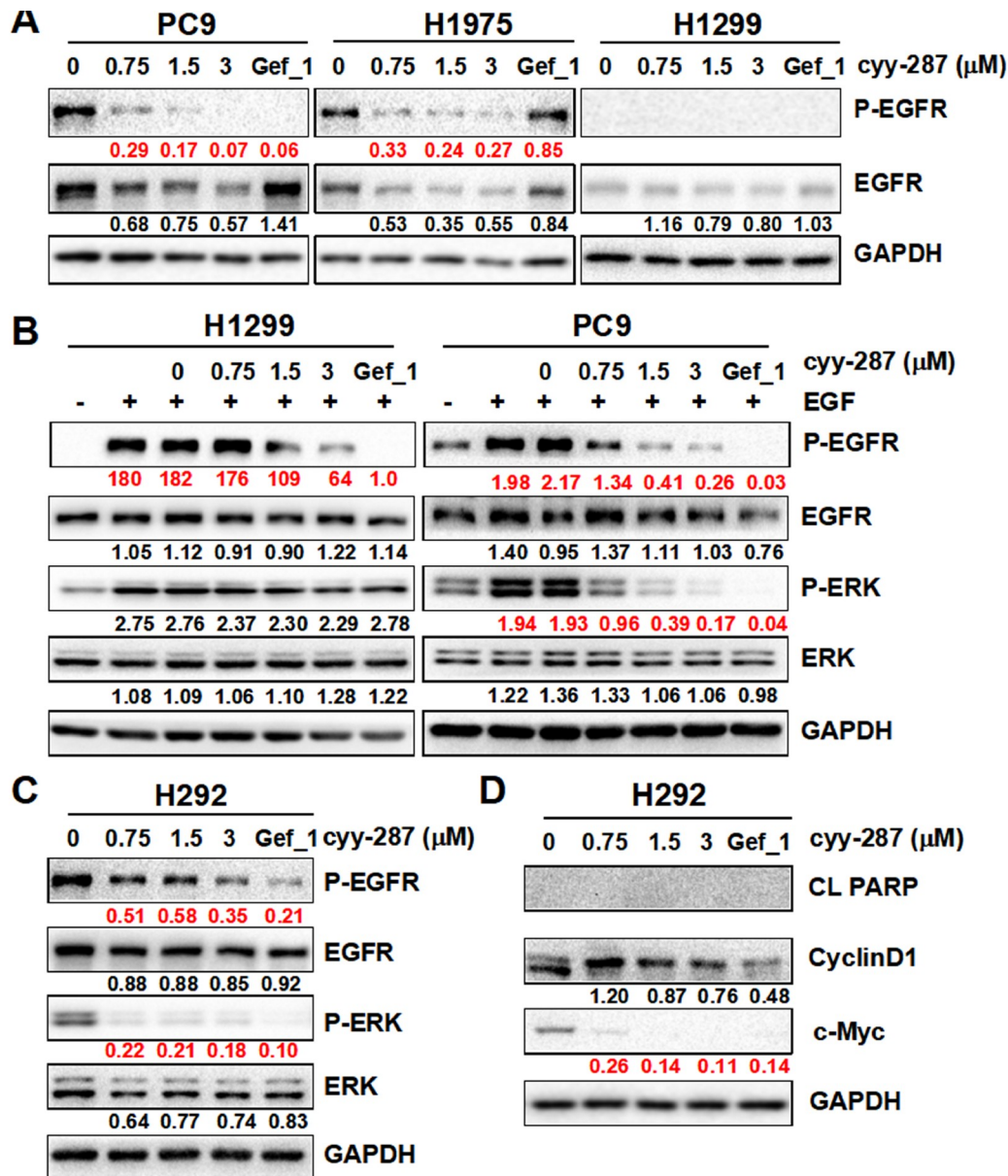
Figure 6. cyy-287 blocks EGFR expression but does not induce cell death in EGFR-wt cells (A) Cells were treated as indicated for 24 h and then subject to western blot analysis. (B) Cells were treated with EGF (100 ng/mL) for 30 min, pretreated with drugs as indicated for 2 h and then subject to western blot analysis. (C) and (D) H292 cells were treated as indicated for 24 h and then subject to western blot analysis. The grayscale value of each blot was quantified.

morphology with cytoskeleton reorganization [18]. The motility, invasiveness, and metastatic ability of tumor cells are closely related to EMT [24]. In a previous study, we demonstrated that blocking the downstream signaling of EGFR is an effective way to inhibit the metastasis and EMT of EGFR-driven NSCLC cells [25]. In the present study, we found that the migration of EGFR-driven NSCLC cells was significantly inhibited by cyy-287 (Figure 3A–D). Meanwhile, the protein expression levels of EMT-related Vimentin and Slug were decreased after cyy-287 treatment (Figure 3E). These results suggest that cyy-287 suppresses the metastasis of EGFR-driven NSCLC cells via EMT inhibition.

Unlike the antiproliferation effect of cyy-287 in human NSCLC cells, cyy-287 only induced cell apoptosis in EGFR-driven NSCLC

cells (Figure 4A,B). As the cyy-287 concentration increased, the number of Annexin V-positive cells and the level of CL-PARP were increased (Figure 4B,C). To determine the underlying mechanisms of cyy-287-induced apoptosis in EGFR-driven NSCLC cells, total RNA from PC9 cells with or without cyy-287 treatment was extracted and sequenced. The sequencing results were subject to KEGG enrichment analysis, and the results showed that cyy-287 treatment significantly inhibited the MAPK signaling pathway in PC9 cells (Figure 5C). These results suggest that the MAPK family is probably involved in cyy-287-induced cell apoptosis in EGFR-driven NSCLC cells.

The ERK pathway is the most important signaling cascade among all MAPK signal transduction pathways and is closely related to the survival and development of tumor cells [26,27]. ERK hyperactiva-
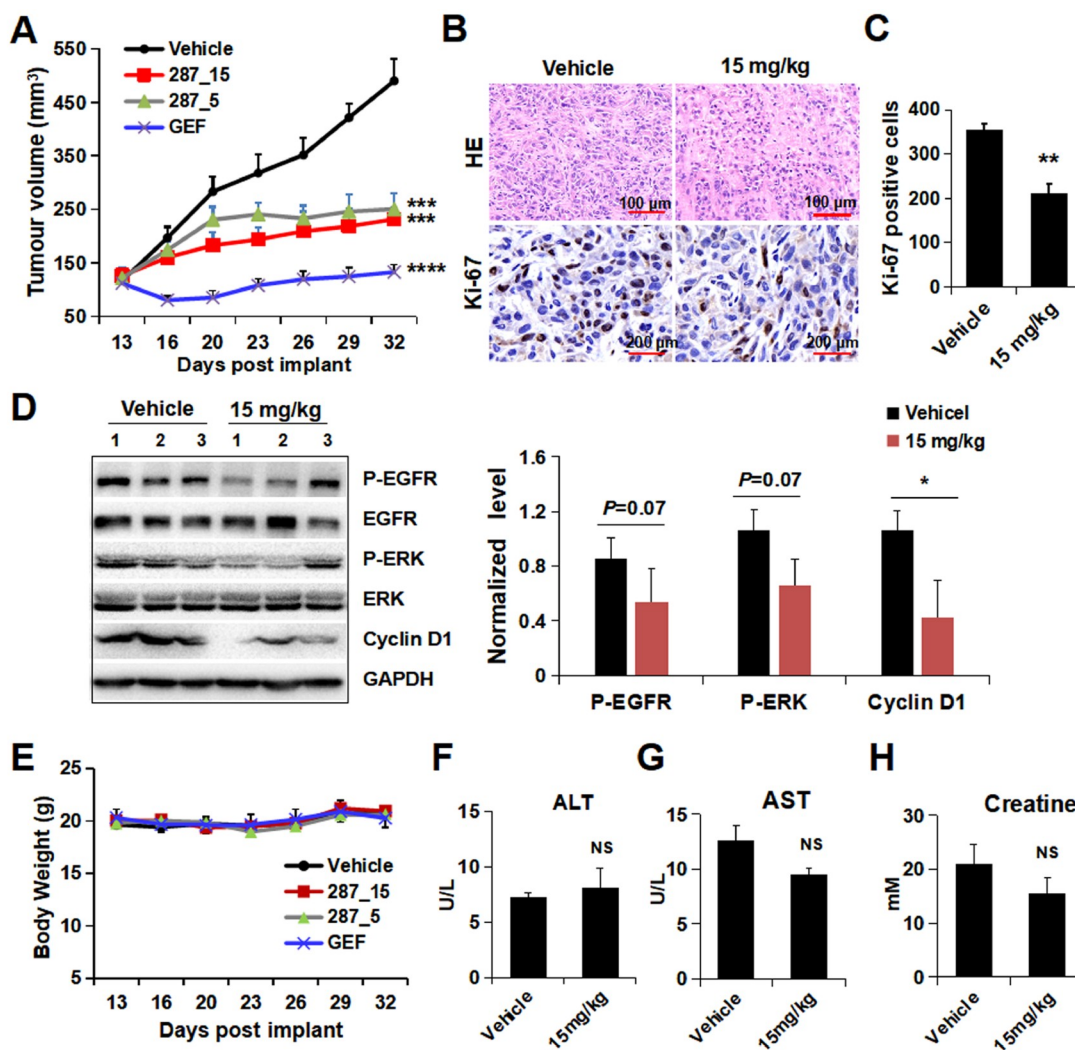
Figure 7. cyy-287 inhibits the *in vivo* tumor growth of PC9 cells Tumor-bearing mice were intraperitoneally injected with vehicle (0.9% saline buffer), cyy-287 (15 mg/kg), cyy-287 (5 mg/kg) or gefitinib (15 mg/kg). (A) Tumor volumes of PC9 human lung cancer xenografts in nude mice. (B) Tumor sections were analysed by HE (scale bar: 100 μm) and IHC using anti-Ki-67 antibody (scale bar: 200 μm). (C) Quantitative data of Ki-67 in (B). (D) Proteins were extracted from tumor sections and then subject to western blot analysis. Quantified results were plotted. (E) Body weights of the tumor-bearing mice. (F–H) Serum levels of ALT, AST and creatinine in mice treated with and without cyy-287 (15 mg/kg). Data are expressed as the mean ± SD ($n = 6$). *$P < 0.05$, **$P < 0.01$, ***$P < 0.001$, ****$P < 0.0001$ compared with the control group. NS, no significance.

tion plays a major role in cancer development and progression, including tumor proliferation, invasion, metastasis, and angiogenesis [28]. In this study, we found that p-ERK was only suppressed in EGFR-driven NSCLC cells after cyy-287 treatment, while p-p38 and p-JNK were inhibited in all three cell lines (Figure 5D). The apoptosis level was decreased when PC9 cells were treated with cyy-287 combined with UO126 (Figure 5G,H), indicating that the ERK pathway is critical for the survival of EGFR-driven NSCLC cells treated with cyy-287. Moreover, although cyy-287 inhibited the protein expression levels of p-EGFR and p-ERK in EGFR-wt H292 cells, it had no effect on cell death (Figure 6C,D). These results suggest that apoptosis induced by cyy-287 is mainly by ERK inhibition in EGFR-driven cells but not in EGFR-wt cells, which also explains why cyy-287 has higher inhibitory efficiency on EGFR-driven NSCLC cells. Studies have revealed that aberrant activation of the ERK pathway is involved in HGF-induced EGFR-TKI

resistance in NSCLC and breast cancer [29,30]. In addition, activation of the Ras/RAF/MEK/ERK pathway may lead to acquired osimertinib resistance in patients with advanced EGFR-mutated NSCLC [31,32]. We found that cyy-287 blocked ERK activation in EGF-stimulated PC9 cells (Figure 6B). However, whether cyy-287 could block ERK phosphorylation stimulated by other cytokines (such as HGF) or induced by Ras/RAF mutation needs further study, which may be a promising method to overcome EGFR-TKI resistance caused by aberrated activation of bypass pathways or abnormal downstream pathways.

In conclusion, we discovered that cyy-287 significantly inhibited tumour growth and proliferation in EGFR-driven NSCLC cells with fewer side effects. In addition, our results also indicated that cyy-287 induced cell cycle arrest in G2/M phase and suppressed migration by EMT inhibition. Meanwhile, cyy-287 treatment promoted apoptosis by blocking the ERK pathway (Figure 8).
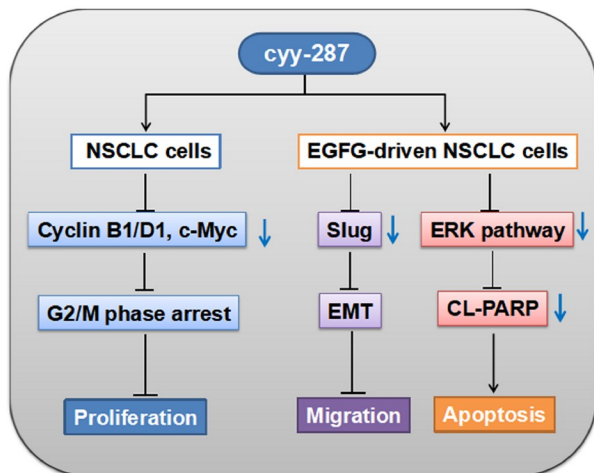
Figure 8. Schematic diagram of the molecular mechanism of the anti-tumour effect of cyy-287 on NSCLC cells cyy-287 inhibits cyclin B1/D1 and c-Myc, induces cell cycle arrest in the G2/M phase. Meanwhile, cyy-287 treatment suppresses the EMT of EGFR-driven cells by Slug inhibition and inhibits ERK signaling, leading to the downregulation of CL-PARP and cell apoptosis.

Overall, this study illustrates that cyy-287 possesses a promising antitumor effect on EGFR-driven NSCLC cells, which provides an experimental basis for the future application of cyy-287 in the clinical treatment of NSCLC.

Supplementary Data

Supplementary data is available at *Acta Biochimica et Biophysica Sinica* online.

Funding

Conflict of Interest

The authors declare that they have no conflict of interest.

References

1. Liang W, Liu J, He J. Driving the improvement of lung cancer prognosis. *Cancer Cell* 2020, 38: 449–451

2. Sung H, Ferlay J, Siegel RL, Laversanne M, Soerjomataram I, Jemal A, Bray F. Global cancer statistics 2020: GLOBOCAN estimates of incidence and mortality worldwide for 36 cancers in 185 countries. *CA Cancer J Clin* 2021, 71: 209–249

3. Chang A. Chemotherapy, chemoresistance and the changing treatment landscape for NSCLC. *Lung Cancer* 2011, 71: 3–10

4. Maity S, Pai KSR, Nayak Y. Advances in targeting EGFR allosteric site as anti-NSCLC therapy to overcome the drug resistance. *Pharmacol Rep* 2020, 72: 799–813

5. Schiller JH, Harrington D, Belani CP, Langer C, Sandler A, Krook J, Zhu J, *et al.* Comparison of four chemotherapy regimens for advanced non–small-cell lung cancer. *N Engl J Med* 2002, 346: 92–98

6. Fossella F, Pereira JR, von Pawel J, Pluzanska A, Gorbounova V, Kaukel E, Mattson KV, *et al.* Randomized, multinational, phase III study of docetaxel plus platinum combinations versus vinorelbine plus cisplatin for advanced non–small-cell lung cancer: the TAX 326 study group. *J Clin Oncol* 2003, 21: 3016–3024

7. Sharma SV, Bell DW, Settleman J, Haber DA. Epidermal growth factor receptor mutations in lung cancer. *Nat Rev Cancer* 2007, 7: 169–181

8. Cataldo VD, Gibbons DL, Pérez-Soler R, Quintás-Cardama A. Treatment of non–small-cell lung cancer with erlotinib or gefitinib. *N Engl J Med* 2011, 364: 947–955

9. Kuang Y, Rogers A, Yeap BY, Wang L, Makrigiorgos M, Vetrand K, Thiede S, *et al.* Noninvasive detection of *EGFR* T790M in gefitinib or erlotinib resistant non–small cell lung cancer. *Clin Cancer Res* 2009, 15: 2630–2636

10. Sutto L, Gervasio FL. Effects of oncogenic mutations on the conformational free-energy landscape of EGFR kinase. *Proc Natl Acad Sci USA* 2013, 110: 10616–10621

11. Thress KS, Paweletz CP, Felip E, Cho BC, Stetson D, Dougherty B, Lai Z, *et al.* Acquired EGFR C797S mutation mediates resistance to AZD9291 in non–small cell lung cancer harboring EGFR T790M. *Nat Med* 2015, 21: 560–562

12. Kwon OJ, Zhang L, Jia D, Zhou Z, Li Z, Haffner M, Lee JK, *et al.* De novo induction of lineage plasticity from human prostate luminal epithelial cells by activated AKT1 and c-Myc. *Oncogene* 2020, 39: 7142–7151

13. Wang K, Ji W, Yu Y, Li Z, Niu X, Xia W, Lu S. Correction: FGFR1-ERK1/2-SOX2 axis promotes cell proliferation, epithelial-mesenchymal transition, and metastasis in FGFR1-amplified lung cancer. *Oncogene* 2020, 39: 6619–6620

14. Lei T, Huang J, Xie F, Gu J, Cheng Z, Wang Z. HMGB1-mediated autophagy promotes gefitinib resistance in human non-small cell lung cancer. *Acta Biochim Biophys Sin* 2022, 54: 514–523

15. Low HB, Zhang Y. Regulatory roles of MAPK phosphatases in cancer. *Immune Netw* 2016, 16: 85–98

16. Johnson GL, Lapadat R. Mitogen-activated protein kinase pathways mediated by ERK, JNK, and p38 protein kinases. *Science* 2002, 298: 1911–1912

17. Zang SZ, Yang YR, Zhao SS, Li YX, Gao XY, Zhong CL. In *silico* insight into EGFR treatment in patients with lung carcinoma and T790M mutations. *Exp Therapeutic Med* 2017, 13: 1735–1740

18. Berx G, Raspé E, Christofori G, Thiery JP, Sleeman JP. Pre-EMTing metastasis? Recapitulation of morphogenetic processes in cancer. *Clin Exp Metastasis* 2007, 24: 587–597

19. Travis WD, Brambilla E, Nicholson AG, Yatabe Y, Austin JHM, Beasley MB, Chirieac LR, *et al.* The 2015 world health organization classification of lung tumors. *J Thoracic Oncol* 2015, 10: 1243–1260

20. Zhou C, Wu YL, Chen G, Feng J, Liu XQ, Wang C, Zhang S, *et al.* Final overall survival results from a randomised, phase III study of erlotinib versus chemotherapy as first-line treatment of EGFR mutation-positive advanced non-small-cell lung cancer (OPTIMAL, CTONG-0802). *Ann Oncol* 2015, 26: 1877–1883

21. Rosell R, Carcereny E, Gervais R, Vergnenegre A, Massuti B, Felip E, Palmero R, *et al.* Erlotinib versus standard chemotherapy as first-line treatment for European patients with advanced EGFR mutation-positive non-small-cell lung cancer (EURTAC): a multicentre, open-label, randomised phase 3 trial. *Lancet Oncol* 2012, 13: 239–246

22. Chai B, Ma Z, Wang X, Xu L, Li Y. Functions of non-coding RNAs in regulating cancer drug targets. *Acta Biochim Biophys Sin* 2022, 54: 279–291

23. Jiang T, Zhou C. Clinical activity of the mutant-selective EGFR inhibitor AZD9291 in patients with EGFR inhibitor-resistant non-small cell lung cancer. *Transl Lung Cancer Res* 2014, 3: 370–372

24. Li L, Li W. Epithelial–mesenchymal transition in human cancer:

Comprehensive reprogramming of metabolism, epigenetics, and differentiation. *Pharmacol Ther* 2015, 150: 33–46

25. Zhang Q, Zhang Y, Chen Y, Qian J, Zhang X, Yu K. A novel mTORC1/2 inhibitor (MTI-31) inhibits tumor growth, epithelial–mesenchymal transition, metastases, and improves antitumor immunity in preclinical models of lung cancer. *Clin Cancer Res* 2019, 25: 3630–3642

26. Kolch W. Coordinating ERK/MAPK signalling through scaffolds and inhibitors. *Nat Rev Mol Cell Biol* 2005, 6: 827–837

27. Khokhlatchev AV, Canagarajah B, Wilsbacher J, Robinson M, Atkinson M, Goldsmith E, Cobb MH. Phosphorylation of the MAP kinase ERK2 promotes its homodimerization and nuclear translocation. *Cell* 1998, 93: 605–615

28. Guo YJ, Pan WW, Liu SB, Shen ZF, Xu Y, Hu LL. ERK/MAPK signalling pathway and tumorigenesis. *Exp Ther Med* 2020, 19: 1997–2007

29. Yano S, Wang W, Li Q, Matsumoto K, Sakurama H, Nakamura T, Ogino H, *et al.* Hepatocyte growth factor induces gefitinib resistance of lung adenocarcinoma with epidermal growth factor receptor–activating mutations. *Cancer Res* 2008, 68: 9479–9487

30. Mueller KL, Madden JM, Zoratti GL, Kuperwasser C, List K, Boerner JL. Fibroblast-secreted hepatocyte growth factor mediates epidermal growth factor receptor tyrosine kinase inhibitor resistance in triple-negative breast cancers through paracrine activation of Met. *Breast Cancer Res* 2012, 14: R104

31. Eberlein CA, Stetson D, Markovets AA, Al-Kadhimi KJ, Lai Z, Fisher PR, Meador CB, *et al.* Acquired resistance to the mutant-selective EGFR inhibitor AZD9291 is associated with increased dependence on RAS signaling in preclinical models. *Cancer Res* 2015, 75: 2489–2500

32. Leonetti A, Sharma S, Minari R, Perego P, Giovannetti E, Tiseo M. Resistance mechanisms to osimertinib in EGFR-mutated non-small cell lung cancer. *Br J Cancer* 2019, 121: 725–737